Frustrated total internal reflection of newton rings multiple beam interference

Qahtan Ghatih Hial

Department of Physics, College of Science, Baghdad University, Baghdad, Iraq

E-mail: qahtan_L84@yahoo.co.uk

Abstract

Frustrated Total Internal Reflection FTIR phenomenon is manifested employing Newton's rings setup generated via a coherent light beam of a laser diode ($\lambda = 532\ nm$). All concentric bright and dark rings, except the central bright spot, were noticed to recede (disappear) when the incident angle exceeded the critical angle of 41^o.

It was also shown that the current setup has proven its applicability for other tests and can give convenient results that conform with theory. Neither the concept nor the design is beyond what can be realized in an undergraduate laboratory. However, technical improvements in mounting the prism - lens may be advisable. As an extension of the experiments, the effect can be studied using hollow prism filled with liquids of different refractive indices for both S and P polarizations of light. Also, the relationship of wavelength on the penetration depth can be explored.

Key words

Frustrated total internal reflection, evanescent waves, total internal reflection, newton rings, multiple – beam interference.

Article info.

Received: Mar. 2017
Accepted: May. 2017
Published: Dec. 2017

الأنعكاس الداخلي الكلي المُثبط لتداخل حلقات نيوتن المتعدد الحزم

قحطان كاطع حيال

قسم الفيزيـــاء، كليـــة العلـــوم، جامعـــة بغـــداد، بغـــداد، العـــراق

الخلاصـــة

يتم تبيان ظاهرة الأنعكاس الداخلي الكلي المُثبط بأستخدام منظومة حلقات نيوتن المتولدة بأستعمال حزمة ضوئية متشاكه للثنائي الليزري (الطول الموجي 532 نانومتر). لقد لوحظ أنحسار (أختفاء) جميع الحلقات المظلمة والمضيئة المتمركزة بأستثناء البقعة المضيئة المركزيۀ عند تجاوز زاوية السقوط الزاوية الحرجة ذات الـ 41 درجة.

أضافة لذلك، بُرهنت قابلية التطبيق للمنظومة الحالية لأجراء االأختبارات الأخرى وأمكانية أعطاء نتائج ملائمة تتفق مع النظري. ورغم كون مبدأ او تصميم التجربة سهل المنال في مختبر الدراسة الأولية، الا أن التحسينات التقنية لتثبيت العدسة – الموشور يمكن أن يُنصح بها. وكأضافة للتجارب الممكن القيام بها هو دراسة هذا التاثير بأستعمال موشور مجوف مملوء بسوائل ذات معاملات أنكسار مختلفة ولكل من الضوء المستقطب S و P. كذلك يمكن بحث علاقة الطول الموجي بعمق الأختراق.

Introduction & principles

Total Internal Reflection TIR

In the usual situation, when light encounters a boundary between two media of different optical densities, i.e., different refractive indexes ($n_i$and n_t) such that $n_i < n_t$ at any angle of incidence θ_i with the normal to the interface, then there will always be a calculable angle of refraction θ_t [1]. Thus, a propagating transmitted wave exists. Snell's law of refraction:

$n_i \sin\theta_i = n_t \sin\theta_t$ is satisfied with a transmitted angle θ_t between 0 and $\pi/2$. But, if $n_t/n_i < 1$, for example when light goes from glass ($n_i = 1.5$) to air ($n_t = 1$), there is no real solution

for θ_t for an angle of incidence $\theta_i \geq \theta_c$. This angle is called the critical angle, and above it light will be total internally reflected (Both polarization reflectance R_s and R_p become unity). This phenomenon is called Total Internal Reflection TIR [1, 2].

Two conditions must be satisfied for TIR to occur:

1. $n_i > n_t$, that is, the incident light wave is in the denser medium.
2. $\theta_i > \theta_c$, that is, the incident angle is greater than the critical angle.

Upon the occurrence of TIR phenomenon, both S (TE) and P (TM) polarizations are 100% reflected, however, they will experience different phase shifts [3]. Actually, total internal reflection is never 100%, as it is accompanied by a wave travelling beyond the boundary called "evanescent wave" [4]. The penetration distance is a few wavelengths and carries no energy unless a third medium of similar optical density is set right beneath the first medium; then appreciable evanescent wave amplitude will cross the gap, giving rise to frustrate the TIR (FTIR phenomenon) [5]. FTIR has many applications in optics including a beam splitter cube made by a thin low index transparent film separating two right angle prisms, Low – pass reflectors with controllable transmittance, scanning optical microscopy, material testing. FTIR will be explored on multiply – reflected interference Newton's rings.

Critical angle θ_c

Critical angle refers to the incident angle for which the refracted angle is exactly π/2. This is a special case that occurs only for internal reflections [1]. To calculate the critical angle θ_c, Snell's law is applied at the interface:

$$n_i \sin\theta_i = n_t \sin\theta_t, \quad (1)$$

Therefore:

$$n_i \sin\theta_c = n_t \sin\frac{\pi}{2}, \quad (2)$$

Or:

$$\theta_c \equiv \sin^{-1}\left(\frac{n_t}{n_i}\right), \quad (3)$$

As an example for a glass – air interface, the critical angle occurs at 41.8^o and for water – air interface, this occurs at 48.8^o.

It is no wonder when someone asks about what Snell's law is going to look like beyond the critical angle.

It can be shown that, even in the case of total internal reflection, Snell's law still holds, except that the sine of the transmitted angle becomes greater than 1, and the cosine of the transmitted angle becomes imaginary. Though there is no physical interpretation of the "transmitted angle", it is still useful as a mathematical tool. The Fresnel reflection formulae for both S and P wave polarizations still apply if we continue to use the $\cos\theta_t$ term, despite its imaginary value.

The equation describing the spatial variation of the electromagnetic wave is:

$$E = E_0 e^{\pm i(k.r)}, \quad (4)$$

The Snell's law is applicable whenever light encounters a boundary between two media [1]:

$$n_i \sin\theta_i = n_t \sin\theta_t, \quad (5)$$

$$\sin\theta_t = \frac{n_i}{n_t}\sin\theta_i \quad \rightarrow \quad \sin\theta_t = \frac{\sin\theta_i}{\sin\theta_c} \quad \rightarrow \quad \sin^2\theta_t = \frac{\sin^2\theta_i}{\sin^2\theta_c}$$

$$1 - \sin^2\theta_t = 1 - \frac{\sin^2\theta_i}{\sin^2\theta_c} \quad \rightarrow$$

$$\cos^2\theta_t = 1 - \frac{\sin^2\theta_i}{\sin^2\theta_c} \quad \rightarrow$$

$$\cos\theta_t = \sqrt{1 - \frac{\sin^2\theta_i}{\sin^2\theta_c}}, \qquad (6)$$

Total internal reflection occurs when:

$$\theta_c < \theta_i < \frac{\pi}{2} \quad \rightarrow \quad \frac{\sin^2\theta_i}{\sin^2\theta_c} > 1,$$

$$\cos\theta_t = \sqrt{-1\left(\frac{\sin^2\theta_i}{\sin^2\theta_c} - 1\right)} \quad \rightarrow$$

$$\cos\theta_t = i\sqrt{\left(\frac{\sin^2\theta_i}{\sin^2\theta_c} - 1\right)}, \qquad (7)$$

$$\rightarrow \quad \cos\theta_t = \pm i\sqrt{\left(\frac{n_i^2}{n_t^2}\sin^2\theta_i - 1\right)}, \qquad (8)$$

Having determined the cosine of θ_t ($\cos\theta_t$) in total internal reflection, one may apply the wave equation to describe the wave that penetrates into the second medium in total internal reflection. To determine the behavior of this wave in the direction d (normal to the surface) a scalar product between k and the position d must be included in the wave equation [5]:

$$E = E_0 e^{\pm ikd(\cos\theta_t)} \quad \rightarrow \quad E = E_0 e^{\pm ikd\left(i\sqrt{\left(\frac{n_i^2}{n_t^2}\sin^2\theta_i - 1\right)}\right)} \quad \rightarrow$$

$$E = E_0 e^{\pm\left[\frac{2\pi}{\lambda}di^2\sqrt{\left(\frac{n_i^2}{n_t^2}\sin^2\theta_i - 1\right)}\right]} \quad \rightarrow \quad E = E_0 e^{\pm[-d\beta]}$$

$$where\ \beta = \frac{2\pi}{\lambda}\sqrt{\left(\frac{n_i^2}{n_t^2}\sin^2\theta_i - 1\right)}, \qquad (9)$$

Two solutions are then available, a positive and a negative exponential:

$$\rightarrow \quad E = E_0 e^{\pm d\beta}, \qquad (10)$$

Evanescent wave

For the sake of conservation of energy, only the negative exponential have to be considered. Thereby, evanescent wave, decays exponentially [6].

Assuming the wave vector k_t of the "transmitted wave" exists and in order to satisfy the wave equations, one must have:

$$|k_t| = \sqrt{k_{tx}^2 + k_{ty}^2} = \frac{\omega}{c}n_t, \qquad (11)$$

and in order to satisfy the boundary phase-matching condition, the following must be valid:

$$k_{tx} = k_{ix} = k_i \sin\theta_i = \frac{\omega}{c} n_i \sin\theta_i, \quad (12)$$

Note that $n_i \sin\theta_i > n_t$ at θ_i beyond the critical angle θ_c, therefore, k_{ty} must become imaginary.

$$k_{ty} = \sqrt{k_t^2 - k_{tx}^2} = \sqrt{k_t^2 - (k_i \sin\theta_i)^2} = \frac{\omega}{c}\sqrt{n_t^2 - n_i^2 \sin^2\theta_i}$$
$$= \frac{\omega}{c}\sqrt{-(n_i^2 \sin^2\theta_i - n_t^2)} = \pm i\frac{\omega}{c} n_t \sqrt{\frac{n_i^2}{n_t^2}\sin^2\theta_i - 1} \quad \rightarrow \quad k_{ty}$$
$$\equiv \pm i\beta, \quad (13)$$

Substituting this imaginary wave vector k_{ty} into the usual wave expression for the transmitted wave will yield the following:

$$E_t = E_{t0} exp\left[i(k_{tx}x + k_{ty}y - \omega t + \varphi)\right] = \underbrace{E_{t0}e^{\beta y}}\ \underbrace{exp\left[i(\frac{\omega}{c} n_i \sin\theta_i\, x - \omega t + \varphi)\right]}$$

The 1st term resembles the exponentially decaying with –y amplitude; whereas the 2nd one represents a wave propagating in the x direction with $v = c/n_i \sin\theta_i$.

Here, only $k_{ty} \equiv -i\beta$ is considered since $k_{ty} \equiv +i\beta$ leads to an unphysical result. The wave expressed by the above equation is a peculiar wave: it differs from the regular plane wave in that its amplitude exponentially decays in the directions orthogonal to its propagation direction. It is called an "Evanescent Wave".

From the equation of E_t, three conclusions regarding the amplitude of the transmitted E field can be drawn [6]:

1. E field is finite in the n_t medium, that is, there is field penetration into the transmitted medium. The field does not stop abruptly at the interface.
2. E field is constant in the planes parallel to the interface, i.e., for y = constant.
3. E field decays exponentially with the distance away from the interface.

Penetration depth

Usually, two penetration depths can be defined:

1) The distance from the interface at which the E field decays to its 1/e value.

Field penetration depth =1/β.

2) The distance from the interface at which the intensity decays to its 1/e value.

Intensity penetration depth =1/2β.

The penetration depth is function of the incident angle at the interface separating the two media and therefore it has a greatest value at grazing incidence, i.e., at $\theta_i = 90^\circ$ [7].

Complex fresnel reflection coefficients

Fresnel reflection coefficients can still be applied to the TIR case, as long as one incorporates the imaginary $\cos\theta_t$ term, expressed by [8]:

$$\cos\theta_t = \pm i\sqrt{\left(\frac{n_i^2}{n_t^2}\sin^2\theta_i - 1\right)}$$

And for both S and P polarizations

- TE case (S polarization):

$$r_{TE} = \frac{n_i \cos\theta_i - i n_t \sqrt{\left(\frac{n_i^2}{n_t^2}\sin^2\theta_i - 1\right)}}{n_i \cos\theta_i + i n_t \sqrt{\left(\frac{n_i^2}{n_t^2}\sin^2\theta_i - 1\right)}} \quad \rightarrow \quad r_{TE} = \frac{a - ib}{a + ib} \quad \rightarrow \quad r_{TE} = e^{i\phi_{TE}}$$

$$\phi_{TE} = -2\tan^{-1}\left(\frac{n_t \sqrt{\left(\frac{n_i^2}{n_t^2}\sin^2\theta_i - 1\right)}}{n_i \cos\theta_i}\right)$$

- TM case (P polarization):

$$r_{TM} = \frac{-n_t \cos\theta_i + i n_i \sqrt{\left(\frac{n_i^2}{n_t^2}\sin^2\theta_i - 1\right)}}{n_t \cos\theta_i + i n_i \sqrt{\left(\frac{n_i^2}{n_t^2}\sin^2\theta_i - 1\right)}} \quad \rightarrow \quad r_{TM} = \frac{a - ib}{a + ib} \quad \rightarrow \quad r_{TM} = e^{i\phi_{TM}}$$

$$\phi_{TM} = -2\tan^{-1}\left(\frac{n_i \sqrt{\left(\frac{n_i^2}{n_t^2}\sin^2\theta_i - 1\right)}}{n_t \cos\theta_i}\right) + \pi$$

From the above equations, the following important points can be emphasized:

1) The wave is 100% reflected;
2) The reflected wave is not in phase with the incident wave;
3) The additional phase incurred in the reflected wave is different from TE and TM polarized waves.

Frustrated Total Internal Reflection FTIR

Even though the evanescent wave does not transport any energy to the n_t medium, the finite E field in the n_t medium can still polarize the atoms in the medium. If a higher index medium with index n_{t2} is placed near the n_i/n_t interface, and as long as the boundary conditions can be satisfied by a propagating wave in the n_{t2} medium, a propagating transmitted wave will result. Consequently, a finite amount of energy will be transmitted to the n_{t2} medium, and it is said that the initial total internal reflection is frustrated (i.e., the reflection is no longer total) and one has the phenomenon of optical tunneling or frustrated total internal reflection FTIR whereby a wave is partially transmitted through a region where it would be forbidden by geometrical optics. This is the electromagnetic equivalent to alpha-particle or electron tunneling in quantum mechanics.

FTIR has been used in numerous applications, including:-

- Prism coupling: coupling light into and out of waveguides;
- Optical directional couplers with variable ratios;
- Coupling light into the "Whisper-Gallery" mode of a high Q resonator

with multiple dielectric layers separated by air gaps, one can create a resonant tunneling condition and make highly selective wavelength filters.

Calculation of the transmittance through the 'forbidden layer' is not difficult, once the effective refractive indices of the media are expressed in terms of $n_i \cos\theta_i$ and $n_t \cos\theta_t$ in the Fresnel's equations for reflectance and transmittance, where clearly the value of $n_t \cos\theta_t$ in the air layer is imaginary. For multilayer calculations, the transmittance T is given by [1, 4, 9]:

$$T = 1 - |r|^2 \quad \rightarrow \quad \frac{1}{T} = \frac{1}{1-|r|^2} = \alpha \sinh^2\left(\frac{\beta d}{2}\right) + \gamma$$

where

$$\beta = \frac{4\pi}{\lambda}\sqrt{\left(\frac{n_i^2}{n_t^2}\sin^2\theta_i - 1\right)}$$

The transmission coefficient near the center of Newton's rings

Newton's rings multiple - beam interference pattern occurs due to the superposition of the light waves reflected from the curved surface of the plano – convex lens and the top surface of the glass plate. Interference of light reflected from any other two surfaces does not occur because the coherence length of conventional sodium lamp, yellow light, is shorter than the optical path between these surfaces.

The center of the interference pattern should be, though not always, dark because a phase shift of 180° occurs when light is reflected by the top surface of the glass plate while no phase shift occurs for the reflection at the curved surface of the lens. The 180° phase shift is due to the boundary condition where light travelling from the rarer medium is reflected by the boundary of the rarer and denser media. To a good approximation, the radius (r_m) of the mth – ordered dark ring is [1, 4]:

$$r_m = \sqrt{mC\lambda} \qquad (14)$$

where C is the radius of curvature of the lens, and λ is the wavelength of light in air.

In essence, the interference pattern with circular fringes is due to the superposition of light waves reflected from a spherical surface and a flat surface. As suggested earlier, if the coherence length of the light source is greater than the thickness of a plano – convex lens, Newton's rings could be observed by superimposing the reflections from the flat and curved surfaces of the lens. A simple way to demonstrate this is to use an ordinary He – Ne laser, whose light has a coherence length of 20 – 30 cm. In this case, the theoretical expression for the radius (R_m) of the dark ring produced with the setup shown in Fig. 1, is given by [10]:

$$R_m = 2D\sqrt{m\lambda/nF} \qquad (15)$$

The result of the derivation indicates that R_m varies directly with D and inversely with $\sqrt{F}$ where D is the distance between the lens and the screen, n is the refractive index of the lens [10].

Apparatus and method

The experimental setup is shown in Fig. 1 below. The light beam from a 10-mW semiconductor laser of wavelength $\lambda = 532\,nm$ is firstly made linearly polarized in either S or P – polarization planes. The polarized beam is then incident on isosceles right angled high quality BK-7 prism (n=1.515) which is mounted on graduated rotating stage. The angle of incidence on the hypotenuse face of the prism is chosen to be only slightly larger than the critical angle of 41.30° to assure a large penetration depth of

the evanescent wave, and thereby reduce the demands for accurate positioning equipment. A bi – convex lens of 10 cm focal length and 5 cm diameter is vertically mounted in close proximity to the hypotenuse face of the prism. The distance of the lens relative to prism can be easily adjusted via a linear stage of 0.01 mm precision. A photo – cell with a digital multimeter (UNI –T 81 B) is used to record the intensity variation of the transmitted (and/or reflected) beam. In order to ensure that the intensity of the light from the laser is constant, the laser should be switched on about half an hour before the experiment is due to start. For accurate results, the measurements should preferably be taken in a darkened room or in constant natural light.

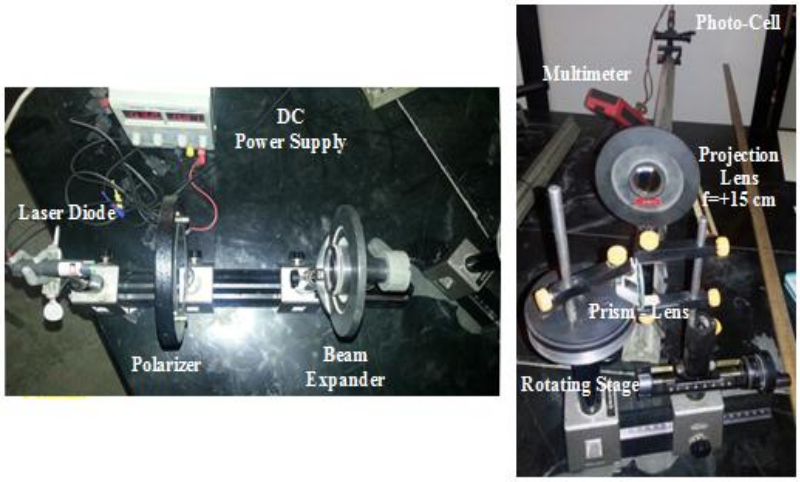

Fig. 1: The experimental setup of the FTIR test.

Newton's rings pattern both by reflection and transmission beams could be observed on white suitable screens. A 15 cm convex lens is employed to project the rings pattern. The reflected beam Newton's rings pattern is identified by a dark spot center. This rings pattern is complementary to its counterpart rings pattern appeared due to transmitted beam where the latter appears with bright spot. Extra care to make the optical components precisely aligned is inevitable. Furthermore, it's worth mention that the prism – convex lens were occasionally required to be cleaned before making the alignment. This step is essential to get a clear and sharp fringe pattern.

Results

Prior to start doing tests, the first thing one has to consider is to assure the perfect contact of the lens convex surface with the prism hypotenuse side. This was done by measuring the ratio of radii of the 2^{nd} – order and 1^{st} – order of either bright or dark Newton's interference rings. Ideally, when the ratio $\frac{r_2}{r_1} = \sqrt{2\lambda R}/\ \sqrt{1\lambda R} \equiv \sqrt{2}$, it indicates the lens is just touching the prism. Upon examining the resulting ring pattern of Fig. 2, the aforementioned procedure has given $\frac{r_2}{r_1}$ radii ratio of 1.4091 and 1.4166 in the transmitted and reflected beams, respectively. This preliminary test was repeated several times and in each one proved the validity ultimate contact between the two surfaces.

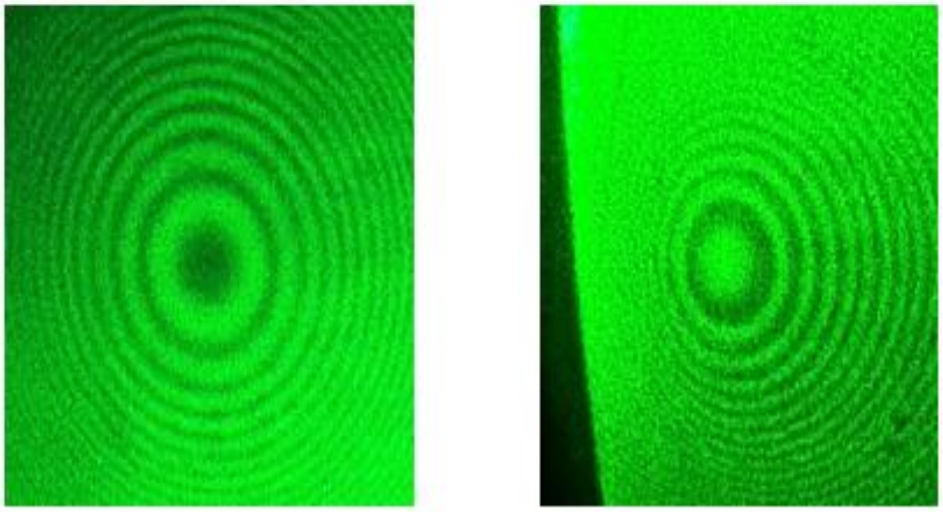

Fig. 2: Newton's rings pattern in the reflected beam (left) and the transmitted beam (right).

Fig. 3 illustrates the pattern of Newton's rings as a series of concentric bright and dark rings resulting from the equal thickness multiple – beam reflection interference. As the incident angle θ_i increases, the rings expand and spread out from the center, Fig. 3 (b-h). As soon as the incident angle θ_i crosses over the critical angle θ_c, all the rings recede from the screen, leaving only a bright spot at the center of Newton's rings, Fig. 3 (i). This spot remains there even if the incident angle has exceeded the critical angle. Fig. 3 (j and l) exhibits receding of Newton's rings in the reflection mode. The remained dark spot here is complement to that in the transmitted mode.

The receding rings and the remaining spot demonstrate the phenomena of frustrated total internal reflection. When the incident angle exceeds the critical angle, total reflection occurs on the convex interface of lens and the incident light is totally reflected, which is why all the rings spread out from the scope and disappear. Because the air film thickness near the center is of the same order as the wavelength of light, total reflection is frustrated there, and light penetrates through this part, which results in the central spot.

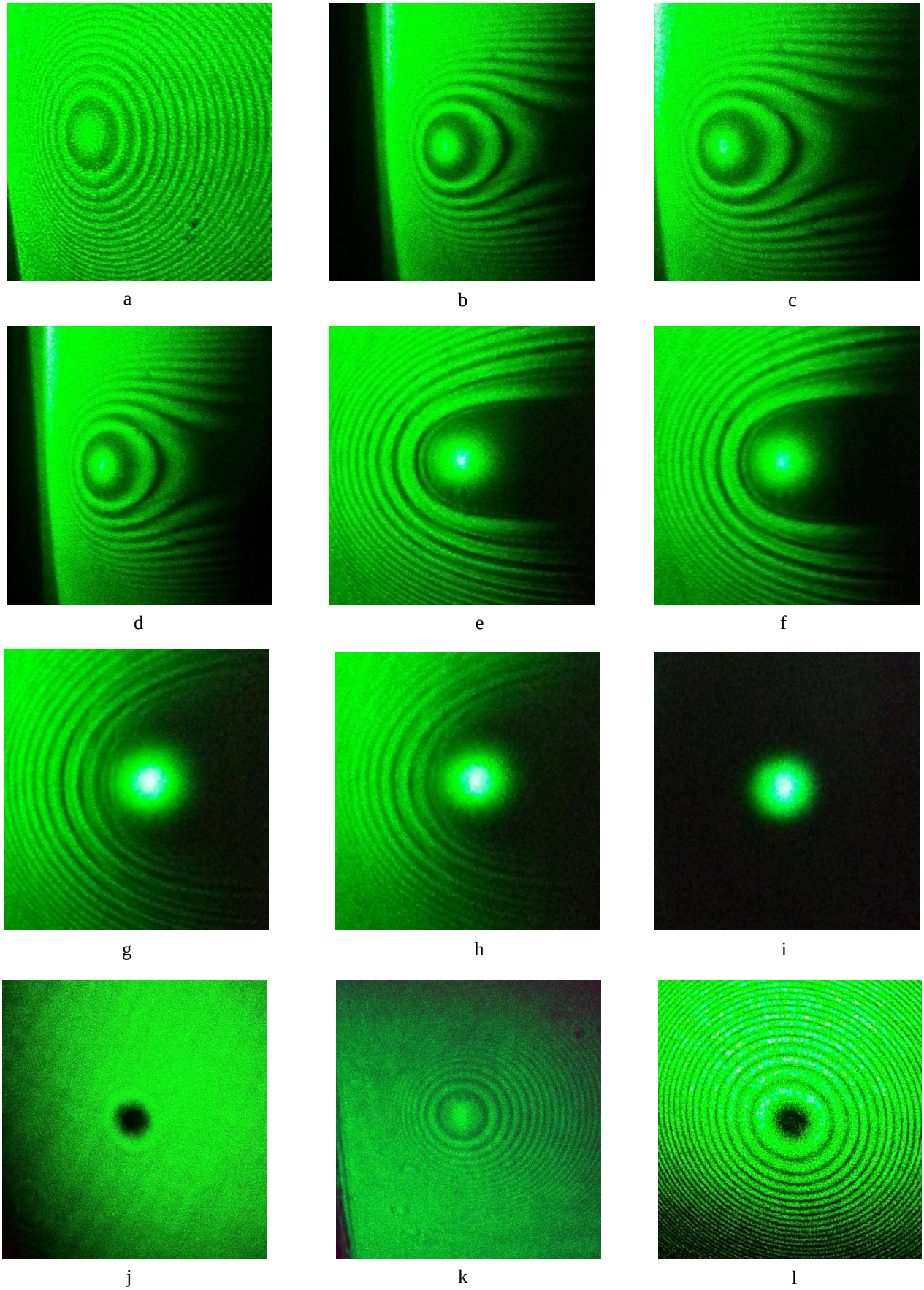

Fig. 3: Receding of Newton's rings in the transmission (a - i) and reflection (j and l) beams upon gradual increasing of the incident angle above the critical angle.

Fig. 4 illustrates the experimental transmitted intensity distribution I of the central spot for both S and P wave polarizations respectively. The lens – photocell distance was at 91.5 cm. The convex lens of +15 cm (quartz) was placed at about 15 cm to the right of the Newton rings system. The diameter of the central spot was around 13.5 to 14 mm. Newton's rings (whether in reflection or transmission beams) disappeared successively upon increasing the incident beam angle at the interface beyond the critical angle θ_c. The bright transmitted spot, that is left at the pattern center due to FTIR occurring at the point of contact, preserved the same appearance and size as that prior to the FTIR. For the Newton rings pattern, the thickness d of the air gap between the lens and the prism changes by $\pm\lambda/2$ between any two successive dark (or bright) ring orders. Since the radius for the 1st bright ring is given by [1]:

$$r_m = \sqrt{m\lambda R} = \sqrt{1 * 532 * 100 \times 10^6} = 230651.2519\ nm$$

$$d_m = \frac{r_m^2}{2R} = \frac{m\lambda R}{2R} = m\frac{\lambda}{2} = 266\ nm$$

Therefore, at the extreme edge of the central spot, the air gap thickness (a measure of the penetration depth) will be around $\lambda/4 \equiv 133\ nm$. Furthermore, this same spot has a diameter of twice the $\lambda/4$ value, i.e., 266 nm. Thereby, the FTIR rays will travel no more than this horizontal distance parallel before returning to the same medium assuming no third medium is present near the boundary.

The bright areas are composed of interference fringes because of the coherent illumination. It should be mentioned here that to avoid extraneous light scattering, great care should be taken to eliminate dust contamination at both the prism and the convex lens, and it proved necessary for us to clean them several times in the course of the experiments.

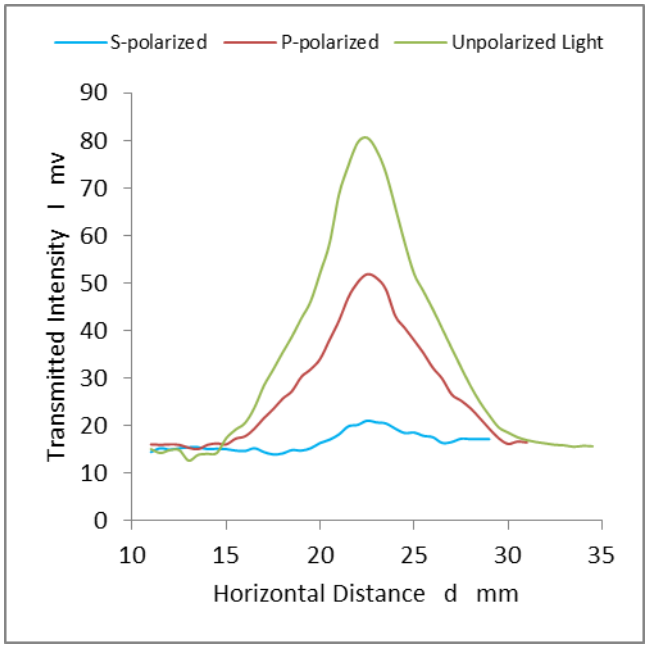

Fig. 4: Transmission intensity variation along the horizontal distance for unpolarized, S- polarized, and P – polarized light, respectively.

Conclusions

In this article, a simple experimental Newton's rings configuration was employed for the demonstration of frustrated total internal reflection phenomenon. The concept and the relatively simple setup prove its reliability and usefulness as an undergraduate optics laboratory experiment. The setup can be used for quantitative measurements and can give good agreement with theory. The receding of the interference rings near the contact point allowed accurate estimation of the critical angle and the penetration depth as well. As an extension of the experiments, the effect can be studied using hollow prism filled with liquids of different refractive indices for both S and P polarizations of light. Also, the relationship of wavelength on the penetration depth can be explored. Finally, it's worth mentioning the importance of the FTIR setup in examining surface plasma on resonance SPR. Such test is currently being undertaken.

Acknowledgements

The author greatly acknowledges assistant professor Dr. Shatha M. Al-Hilly for the unlimited continuous technical support as well as, the opportunity to conduct the experimental tests at the optics lab.

References

[1] E. Hecht, Optics, Addison-Wesley, San Francisco, CA, (2001) 4th Ed.

[2] S. Zhu, A. W. Yu, D. Hawley, R. Roy, Am. J. Phys. 54 (1986) 601–607.

[3] R. M. A. Azzam, J. Opt. Soc. Am. A/ 23, 4, April (2006) 960-965.

[4] Lipson, S. G. Lipson, H. Lipson, Optical Physics, Cambridge University Press, (2011), 4th Ed.

[5] De Fornel, F. Evanescent Waves, From Newtonian Optics to Atomic Optics, Springer Series in Optical Sciences, Springer-Verlag Berlin Heidelberg, (2001) Vol. 73.

[6] Bechara A. Raad and Ira Jacobs, IEEE Transactions on Education, 35, 2, May (1992).

[7] Zoltán Vörös and Rainer Johnsen, Am. J. Phys. 76, 8, August (2008).

[8] Y. You, X. Wang, S. Wang, Y. Pan, J. Zhou: Am. J. Phys. 76, (2008) 224-228.

[9] I. Court and F. K. von Willisen, Appl. Opt. 3 (1964) 719-726

[10] A. F. Leung and Jiyeon Ester Lee, Am. J. Phys., 59 (1991) 662-664.